Annual Report 2000

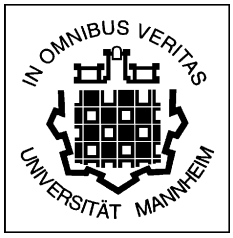

Chair of Optoelectronics
Institute of Computer Science
Faculty of Mathematics and Computer Science
University of Mannheim
B6,23 – 29 Building C
D - 68131 Mannheim
Telephone +49 (0)621 / 181 - 2704
Fax +49 (0)621 / 181 - 2695
EMail info@oe.ti.uni-mannheim.de
WWW http://www.ti.uni-mannheim.de/~oe

We have moved

The most significant change in the year 2000 is that we finally have moved into a new building, which was completed at the side of the old building. Also, the clean room and the optics laboratories were moved into the basement of this building and we thank the transport firm for safely transferring the heavy equipment and the laser tables to their new location. So after 4 years in Mannheim, the offices and the laboratories are finally in one building.
Our research is centered on optical interconnects and optical storage. For these applications, the design and fabrication of micro optical components is the main component of our activities. The masked ion-exchange in glass meanwhile has found an application, which is both scientifically and economically challenging. To this end, a spin-off firm (Brenner & Bähr GdbR) has been founded. Contributions 1 and 2 describe that we have fabricated an array of rectangular micro lenses with diffraction limited performance. These lenses are used in a Hartmann-Shack wavefront sensor. As Robert Klug has finished his PhD-thesis, the work on angle division multiplexing was completed and the studies in contribution 3-6 report on that.
As an industrial development project, the design of micro optics for the pickup of next generation DVD readers poses a series of interesting physical and optical problems. The beam shaping problem described in 7 is still under development and a patent application for the nonsymmetric case has been issued recently. In contribution 8 we have realized a diffractive optical element and in 9 a vectorial treatment of high-NA focussing was performed.

Karl Heinz Brenner

Members of the chair of Optoelectronics

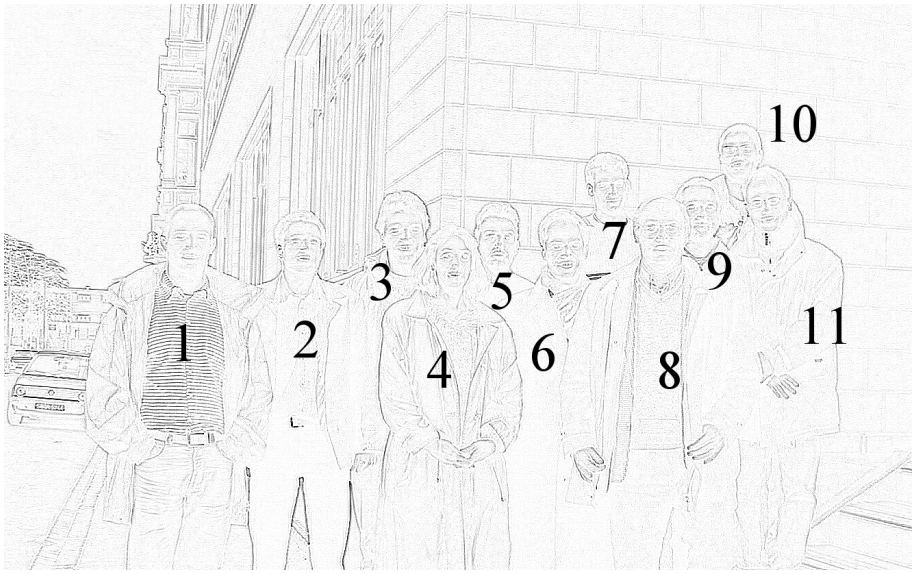

1	Dr. Bähr	Jochen	2694	jb@oe.ti.uni-mannheim.de
8	Prof. Dr. Brenner	Karl-Heinz	2700	brenner@uni-mannheim.de
9	Ehrbächer	Ulrich	2693	uehrbaec@oe.ti.uni-mannheim.de
11	Fauland	Michael		fauland@rumms.uni-mannheim.de
	Flammuth	Sven		flammuth@rumms.uni-mannheim.de
7	Fröning	Holger		maddock@rumms.uni-mannheim.de
	Klug	Robert	2698	klug@opsira.de
6	Dr. Krackhardt	Ulrich	2692	krackhdt@rumms.uni-mannheim.de
10	Kraft	Michael	2702	kraft@oe.ti.uni-mannheim.de
2	Kümmel	Peter	2701	kuemmel@rumms.uni-mannheim.de
	Oberhöffken	Arndt		wwwadmin@oe.ti.uni-mannheim.de
3	Schmelcher	Thilo	2693	t.schmelcher@oe.ti.uni-mannheim.de
	Schulze	Jens		schulze.js@t-online.de
4	Volk	Sabine	2704	office@oe.ti.uni-mannheim.de
5	Walze	Günther	2698	walze@oe.ti.uni-mannheim.de

Contents

1 High precision micro-lenses for Hartmann-Shack wave front sensoring for applications in ophthalmology

J. Bähr, K.-H. Brenner

We report the realization of diffraction limited micro lenses with high fill factor using the mask structured ion exchange process (MSI) for applications in modern ophthalmology. As described in the last annual report, the MSI technique provides a very accurate local insertion of silver ions in planar glass substrates using an exchange mask with locally varying aperture density. With this method diffraction limited performance better than $\lambda/10$ can be achieved at numerical apertures of $N.A. = 0.05$ and less. As an important benefit these types of lenses can be realized with almost arbitrary shape at a fill factor of nearly 100 %. Here we report the realization of quadratic micro lenses in a cartesian pattern.

In modern refractive eye surgery, even high order optical aberrations of the human eye can be corrected almost completely with the LASIK ® technique. According to the measured wave front defects, the cornea of the eye is altered by the use of laser ablation in this method. To identify all kinds of optical defects, the complete optical system of the human eye consisting of cornea, eye-lens and retina has to be examined together. Since the retina scatters light diffusely, the measurement has to be performed incoherently. Figure 1 demonstrates the principle of the measurement. A small spot is generated on the retina by a laser beam. The light scattered back passes the complete optical system of the human eye. In absence of aberrations the eye would act as an ideal collimator. Any wave front errors of the eye can be detected as a deviation form a plane wave, using a wave front detector, here in particular a Hartmann-Shack sensor.

To cover the whole pupil of the human eye an array of 25 x 25 micro lenses with a focal length of 32.0 *mm* and a diameter of 400 μm (fig. 2) is used in the Hartmann-Shack sensor. To minimize the exposure of the eye with the laser beam, the lenses have to provide high efficiency. For this reason the lenses were designed with a quadratic shape demonstrated in fig. 3. Since the mask is realized by a photolithographic process, the positions of the lens centers and also the positions of the spots in the focal plane are as accurate as the laser lithography. Fig. 4 shows the intensity distribution in the focal plane using a plane wave for illumination.

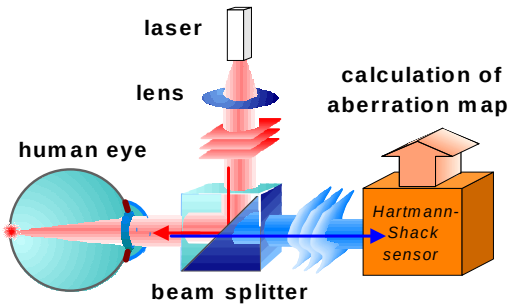

Fig. 1 principle of wave front measurement of the human eye with a Hartmann-Shack sensor

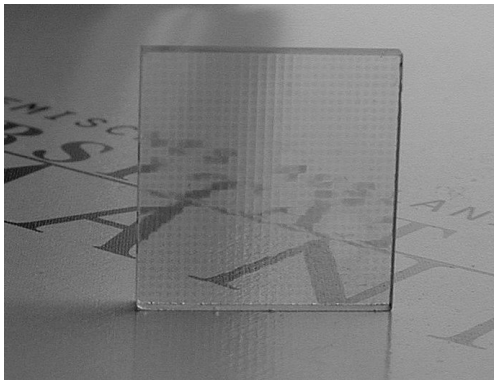

Fig. 2 view of the micro lens array

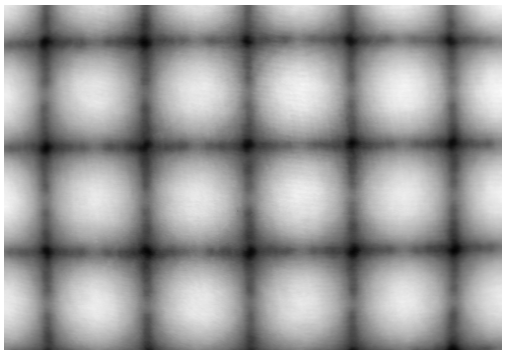

Fig. 3 phase distribution of the lens array

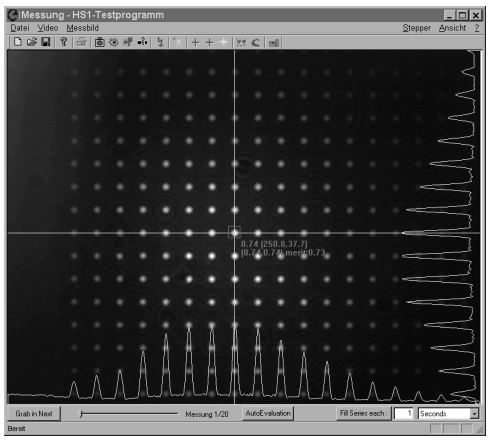

Fig. 4 focal plane and line scan through the array

cooperation partners: 20/10 Perfect Vison GmbH (Heidelberg), VISX Inc. S. Clara (CA, USA), GdbR Brenner und Bähr (Mannheim)

2 Array test of micro lenses for use within Hartman/Shack- sensors

U. W. Krackhardt

The Hartmann/Shack technique provides a metrology of phase fronts without requiring a reference wave [1]. The method is based on the sampling of an input wave front by an array of lenses with a common focal plane (fig. 1). In the case of a plane wave impinging perpendicularly onto the lens array the foci form a regular spot pattern in the focal plane. Any deviation of this wave front results in a shift of the individual foci which corresponds to the average slope of the phase front across a lens cross section.
For automated inspection the ideal spot pattern must be known as exact as possible. Some algorithms are Fourier-based and require a definite periodicity of the ideal spot pattern. Besides the optical quality requirements the lens position is a vital quality criterion for the fabrication of -lens arrays for Hartmann/Shack applications [2].

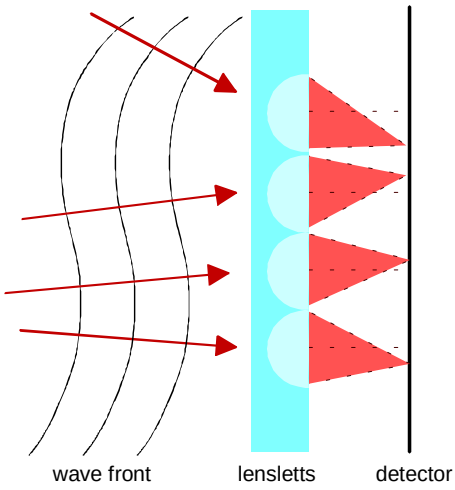

Fig. 1: Sketch of the Hartmann/Shack sensor principle

We have developed a software which is capable of grabbing an image of the focal plane by means of a CCD camera, finding the centers of an arbitrary spot distribution and calculating the relative encircled energy of the spots.
In the image a threshold may be defined interactively to separate the background (ambient and scattered light). Subsequently, a region of interest (ROI) may be defined. Within this ROI the software automatically finds all spots and determines the center of gravity (COG) of each spot. The COG is calculated by an intensity weighted average process thus achieving sub-pixel resolution of typically $1/3, \ldots, 1/5$ of a pixel. In the same step, the encircled energy of each spot is calculated in arbitrary units which serves for judging the homogeneity of the spot array, i.e. the lens transmittivity. The results are presented in a table which may be exported, e.g., to a spread sheet software for further evaluation (fig. 2). The position information may be displayed in absolute units, provided that the system software/camera has been calibrated before.

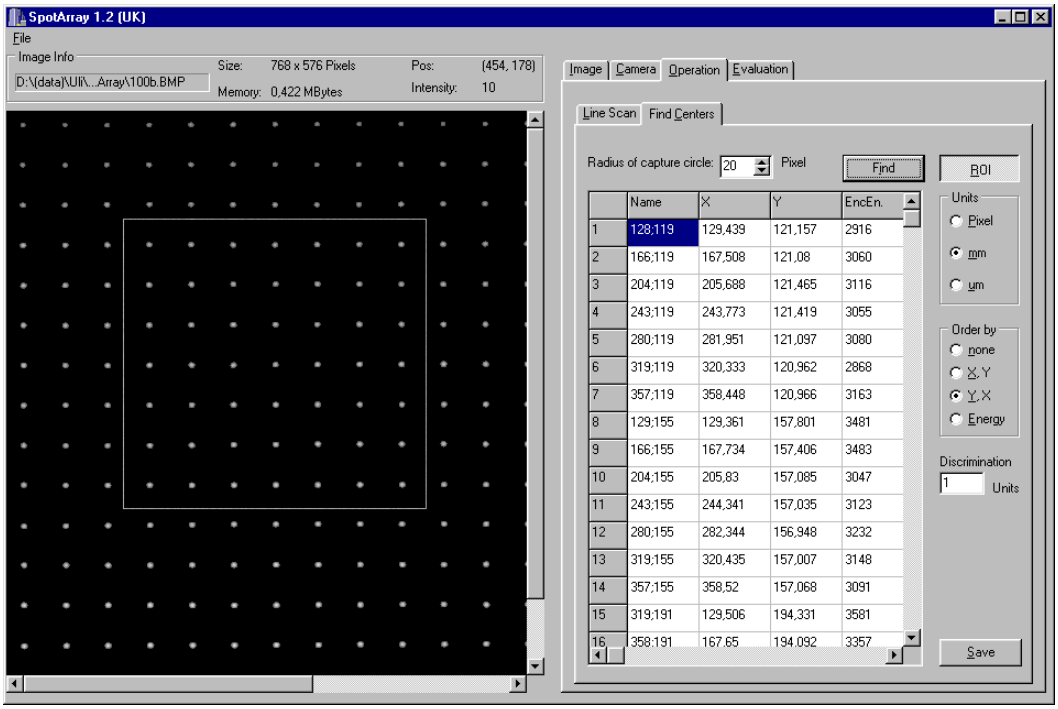

Fig. 2: GUI of the characterization software (Image with ROI and table of results)

References

[1] J.Ghozeil, Hartmann and other screen tests. in Optical Shop Testing, D. Malacara ed., John Whiley, NY (1992)
[2] J. Bähr, High precision micro-lenses for Hartmann-Shack wave front sensoring for applications in ophthalmology. page 4 this report.

3 Exploring the extensibility of the ADM concept

U. W. Krackhardt, S. M. Flammuth

Angle division multiplexing (ADM) allows for multiplexed signal transmission through optical fibers over short distances in the order of several meters [3]. Its suitability for practical applications has been shown in terms of multiplex degree, bandwidth, cross talk, transmission distance, alignment tolerance of MUX and DeMUX units, and robustness against environmental stress. The scope of this contribution is to sketch approaches for extending the ADM concept. Extensions can be thought of in two terms:

- Performance: As described in [4] performance can be measured in terms of the product of the number of logic channels N, the transmission distance L and the cross-talk. The key parameter is the angular extent $\delta\vartheta$ of a channel. A minimum $\delta\vartheta$ leads to a maximum performance. $\delta\vartheta$ consists of a constant offset and a length dependent contribution. The latter is phenomenologically expressed by the mode coupling constant D [4]. The constant offset of $\delta\vartheta$ is due to the angular spectrum of the light source, diffraction at the fiber aperture and scattering due to roughness of the coupling interfaces.
  In order to decrease the constant offset of $\delta\vartheta$ pursued the approach of elevating the influence of the roughness of the coupling interfaces by index matching.

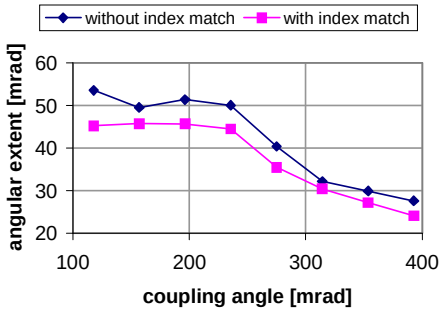

Fig. 1 Angular width vs. coupling angle for a fiber of $L = 7.88\ m$

  To this end, the fiber input has been covered by UV-induced adhesive which matches the core index. Fig. 1 shows that $\delta\vartheta$ can be reduced by a factor of ≈ 1.2 by this technique. It should be noted that this technique can be applied very simply and therefore does not substantially increase fabrication costs. We furthermore investigated polarization properties of the fiber channel. For a fiber length of $L = 0.4\ m$ we measured a polarization contrast of 0.3. For $L = 2\ m$ of the same type of fiber the polarization information was completely lost. Furthermore, polarization is very sensitive to environmental stress like local pressure and bending, i.e. micro and macro bending. As a result of these measurements, the polarization degree of freedom can not be exploited for ADM.

- Handling: Typical applications of ADM are board-to-board, rack-to-rack interconnection and sensor signal transmission. Besides robustness, the effort for mounting an ADM sub-system into an embedding system is decisive for its acceptance. Mounting effort is closely related to the question of connection interfaces. A typical ADM system consists of a MUX and DeMUX module and a multimode step-index fiber. Connection interfaces may be situated either (a) after / before the MUX / DeMUX modules, respectively, or (b) at the multimode step-index fiber. A connection interface within the MUX and DeMUX modules is not suitable due to the alignment requirements of typically $5 - 10\ m$. Approach (a) is a purely electric interconnect, whereas (b) is a purely optical one. We explored approach (b) in terms of power loss due to misalignment. The question of cross-talk is still under investigation. The multimode fiber has been cut into two pieces and butt-coupled again with some controlled misalignment. The misalignment has been realized in terms of lateral shift and tilt. As can be read off from fig. 2 (fiber NA = 0.39), power loss is not a critical parameter since typical fabrication tolerances are 10 μm for lateral shift and 5 *mrad* for tilt control.

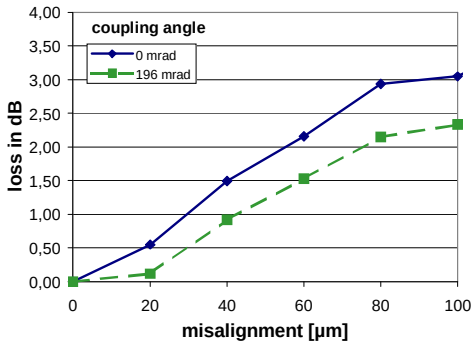

Fig. 2a Power loss due to lateral misalignment

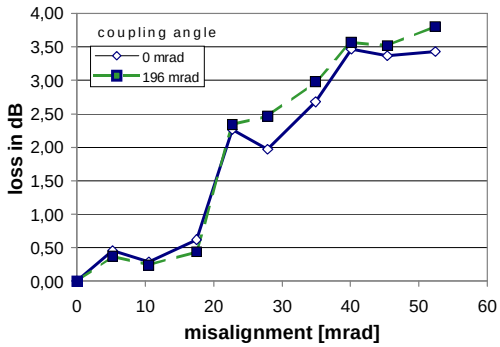

Fig. 2b Power loss due to angular misalignment

References

[3] U.W. Krackhardt, R. Klug and K.-H. Brennerr. Broadband parallel-fiber optical link for short-distance interconnection with multimode fibers. *Appl. Opt.*, **39**, 690–697 (2000)

[4] U. W. Krackhardt, S. M. Flammuth, Automated Measurement of Fiber Quality for Angle Division Multiplexing Applications, 2000. page 7, this report.

4 Automated measurement of fiber quality for Angle Division Multiplexing applications

U. W. Krackhardt, S. M. Flammuth

Angle division multiplexing (ADM) provides a means for parallel data transmission with high aggregate bandwidth through a single multimode step-index fiber [3]. The performance of an ADM system can be measured in terms of the product of the number of logic channels N, the transmission distance L and the cross-talk. It can be shown that optimizing the performance basically is equivalent to minimizing the angular extend per channel $\delta\vartheta_k$. The achievable number of channels is determined by

$$\sum_{k=1}^{N} \delta\vartheta_k \leq \arcsin(NA) \quad \text{where } NA \text{ denotes the fiber NA.}$$

In a real system the value of $\delta\vartheta_k$ is limited by the angular spectrum of the light source, diffraction at the fiber aperture, scattering due to roughness of the coupling interfaces, due to core/cladding imperfections and due to core inhomogeneities. The latter two effects scale with the length of the fiber, i.e. the transmission distance L. These effects cause mode coupling resulting in angular broadening while light propagates through the step-index fiber. Gloge [5] has described the effect of mode coupling in terms of a phenomenological optical power flow analysis. As a result, optical power is distributed around the principal propagation angle by a diffusion-like process. In this context the diffusion constant D describes the effect of mode coupling and is called coupling constant. The angular distribution of the optical power $p(\theta,z)$ is approximately gaussian shaped like

$$p(\theta,z) \propto \exp\left(-\frac{(\theta-\theta_m)^2}{4D\cdot z}\right)\cdot\sqrt{\frac{2D\cdot z}{\theta_m\theta}}$$

, where the letter θ denotes angles within the fiber. θ_m represents the principal propagation direction.

In the far field of the fiber output an angular distribution $\hat{p}(\vartheta)$ can be observed (fig. 1). $\delta\vartheta$ is obtained from $\hat{p}(\vartheta)$ by clipping at an appropriate threshold which is given by the cross-talk requirements. It can be shown [3] that clipping at the $1/e$-level results in a cross-talk of $-10\ dB$ between adjacent channels. Then, $\delta\vartheta \approx \sqrt{4D\cdot z}$. Thus, D can be obtained from linear data fitting of $\delta\vartheta^2$ vs. fiber length z.
We developed a software which acquires the far-field intensity of a multimode step-index fiber at different coupling angles and fiber lengths in an optical set-up described in [6]. From this data $\delta\vartheta$ is obtained by measuring the thickness of the annular rings (fig. 1) and taking into account the geometrical parameters of the measurement set-up. The ring parameters are calculated by image processing and non-linear data fitting (Levenberg-Marquardt). As a result, for each coupling angle ϑ a value of the coupling constant D is obtained (fig. 3).

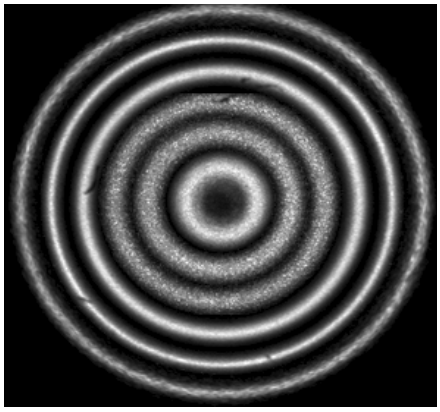

Fig. 1 Far field distribution of a multimode step-index fiber with several active channels

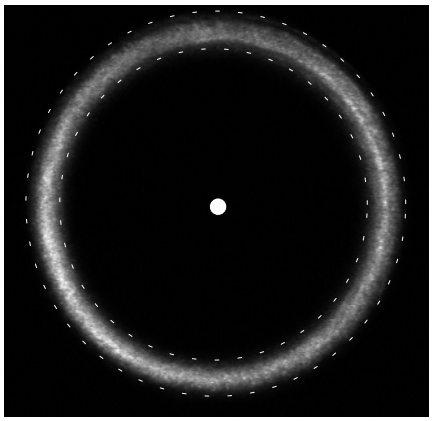

Fig. 2 Automated identification of ring location, radius and thickness by image processing and non-linear data fitting.

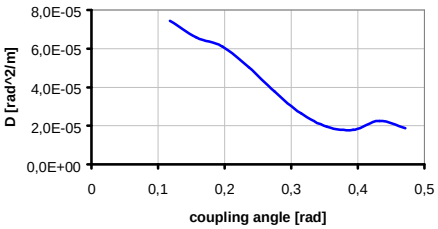

Fig. 3 Result: Coupling constant D vs. coupling angle ϑ

References

[3] U.W. Krackhardt, R. Klug and K.-H. Brennerr. Broadband parallel-fiber optical link for short-distance interconnection with multimode fibers. *Appl. Opt.*, **39**, 690–697 (2000)
[5] D. Gloge. Optical power flow in multimode fibers. *Bell Syst. Techn. J.*, **51**, 1767–1783 (1972)
[6] R.Klug, U.W. Krackhardt, and H. Froening, Design of the demux unit for adm–based interconnects, 1999. page 12, Annual Report 1999.

5 Influence of a Gaussian wave front on the angular spread through multimode step-index fibers

R. Klug, U. W. Krackhardt

Recently, a fiber based multiplexed transmission by angle division multiplexing (ADM) has been proposed [3]. A key parameter of ADM is the angular extent $\delta\vartheta$ of a channel since this limits the performance. The performance of an ADM system may be defined as the product of fiber length L, number of channels N and the maximum tolerable cross-talk.

$\delta\vartheta$ is determined by the angular spectrum of the light coupled into the fiber, diffraction at the fiber apertures, roughness of the coupling interfaces, core inhomogeneities, roughness of the core/cladding interface. The influence of imperfections within a fiber has been described by a phenomenological theory [5].

This contribution investigates the influence of the angular spectrum of the light coupled into the fiber on the angular spectrum of the light coupled out of the fiber. Fig. 1 shows a typical multiplexing (MUX) unit coupling different physical channels into one multimode fiber (MUF) at different coupling angles. The MUX unit images the angular spectrum of the light sources, e.g. VCSELs, onto the fiber input. Provided the light source shows a gaussian angular spectrum there will be a scaled gaussian angular spectrum at the fiber input. The scaling is determined by the magnification of the imaging system. The spectrum at the fiber output is measured in the far field of the fiber aperture in terms of the width of annular rings as described in the last year's annual report [7].

At first glance there are two ways to minimize $\delta\vartheta$: a) Maximum magnification β of the MUX unit. b) Location of the fiber input aperture at the waist of the gaussian beam to have zero curvature at the interface.

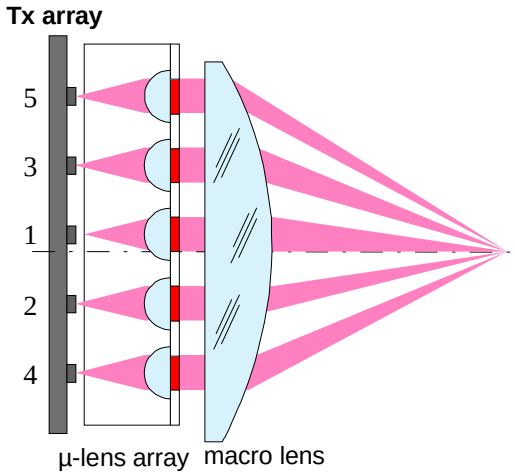

Fig. 1 Sketch of a multiplexing unit

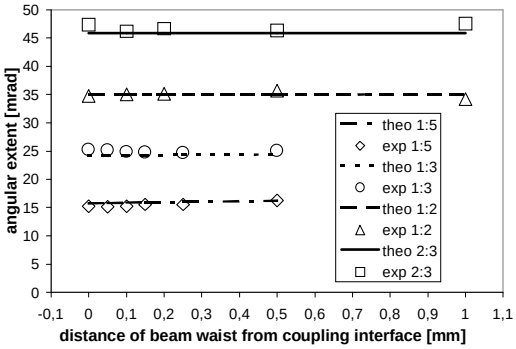

Fig. 2 Angular width vs. distance between fiber aperture and beam waist for different magnifications

Approach a) is limited by the coupling efficiency. Typically, $1 \leq \beta \leq 10$. As can be seen from fig. 2 there is in fact a reduction of angular spread with increasing magnification. The markers indicate experimental results taken from a fiber with $NA = 0.39$ and a core diameter of $d = 200\ \mu m$ and a monomode fiber with $NA = 0.095$ as light source. The solid lines denote theoretical values. The theoretical values are obtained by the consideration that the total gaussian width σ is obtained by a convolution of two gaussians at the fiber output: One gaussian (σ_p) results from a plane wave coupled in, the second gaussian results from the angular spectrum (σ_g) of the input wave front. As a result, $\sigma^2 = \sigma_p^2 + \sigma_g^2$. σ_p is measured by coupling a plane wave, i.e. gaussian beam with a very large radius of curvature, into the fiber. The deviation of experimental from theoretical values are within the resolution of the measurement set-up $(\pm 0.5\ mrad)$.

Likewise, fig. 2 shows that approach (b) is not valid: The angular width $\delta\vartheta$ at the fiber output is virtually independent of the distance between the fiber aperture and the beam waist. This is due to the quasi continuous modal spectrum of the fiber. Therefore, the angular spectrum of a gaussian beam remains constant with free space propagation. In this context, approach (a) corresponds to a hard-clip of the angular spectrum of a gaussian beam, limited by energy loss considerations.

As a result, longitudinal misalignment of the multimode fiber has no impact on the angular width of a channel.

References

[3] U.W. Krackhardt, R. Klug and K.-H. Brenner. Broadband parallel-fiber optical link for short-distance interconnection with multimode fibers. *Appl. Opt.*, **39**, 690–697 (2000)

[5] G. Glode. Optical power flow in multimode fibers. *Bell Syst. Techn. J.*, **51**, 1767–1783 (1972)

[7] R.Klug, U.W. Krackhardt, and K.-H. Brenner, Characterization of Fiber Parameters for Angle Division Multiplexing. page 13 Annual Report of the Chair of Optoelectronics, University of Mannheim, Germany, 13, (1999).

6 Analysis of alignment tolerances of ADM MUX- and DeMUX- modules

R. Klug, U. W. Krackhardt

ADM has been proposed as a fiber-based multiplexed transmission system using Angle Division Multiplexing [3]. Fig. 1 shows typical set-ups for multiplexing (MUX) and de-multiplexing (DeMUX) units. This contribution focuses on the impact of misalignment on the system performance.

A lateral shift of an input source or of a micro-lens in the MUX module (fig. 1) causes a magnified (β_1) lateral shift of the image at the fiber input, thus increasing insertion loss. The same is true for an axial shift, however, scaled by β_1^2 at the fiber input. On the other hand, as discussed in [8], if the fiber input selects only the central part of the beam cross section, a reduced angular spectrum results. The axial shift of the beam waist has virtually no effect to the angular spectrum. As a result, there is a trade-off between insertion loss and angular spectrum for the choice of β_1. The magnification (β_2) of the DeMUX module is limited by two effects: An upper limit is imposed by alignment considerations, i.e., the image of a channel has to stay within the area of a detector in case of lateral misalignment. A lower limit is given by the detector extent and the maximum deflection angle of the CGH (fig. 1). Since the core diameter of the multimode step-index fiber we used is $d = 20\ \mu m$, and the diameter of typical detectors is in the range of $d' \approx 200\ \mu m$, $\beta_2 = 1$ is chosen for a test system. An axial misalignment of the fiber output results in a change of ring radii at the CGH resulting in cross talk. The problem of power insertion into the receivers is considered minor, since the optoelectronic receivers accept virtually all reasonable aperture angles without change of insertion loss.

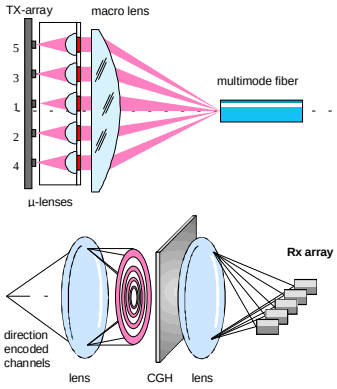

Fig. 1: Typical set-ups for MUX and DeMUX modules

For a quantitative estimation of the influence of fabrication tolerances a 3D, non-paraxial ray tracing formalism has been developed analytically. Since the problem is non-linear, numerical results are now discussed by means of particular design goals: The ADM system is designed to have $N = 10$ channels, an overall cross talk of $-10\ dB$, a detector pitch of 250 μm and a CGH with a maximum deflection angle of 25^o at $\lambda = 850\ nm$. The input sources are monomode fibers with a core diameter of 9 μm. A magnification of $\beta_1 = 10$ is chosen.

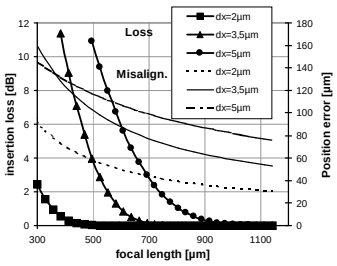

Fig. 2: Loss and misalignment at the MUX unit (see text)

Fig. 2 shows the insertion loss vs. focal length f_1 of the micro lens array for different values of fabrication accuracy dx. For $dx = \pm 3.5 \mu m$ and $f_1 = 575$ there is an insertion loss of $\approx 1.5\ dB$ due to a position mismatch at the fiber input of about 90 μm. The cross talk caused by this MUX unit can be read off from fig. 3 as $-10.7\ dB$. The divergence of the Gaussian beam at the fiber input is 7 $mrad$.

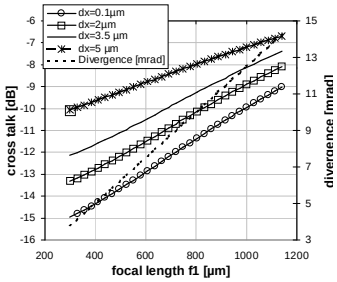

Fig. 3: Beam divergence at the fiber input and cross talk caused by the MUX unit (see text)

As already pointed out, insertion loss is not critical for the design of the DeMUX module. A linear detector array with 10 elements of pitch 250 μm results in $f_3 = f_4 \approx 2.7\ mm$ (fig. 1). Fig. 4 shows the impact of fabrication tolerance on the cross talk: The mismatch of the ring thickness is much less critical than the decentering of the CGH. A decentering of $dx = \pm 7 \mu m$ leads to a degradation of cross talk by 1.5 dB. The overall cross talk of the system with the given design and tolerance data is $-9.9\ dB$. The power loss caused by the MUX and DeMUX units is 1.5 dB (MUX) $+0.7\ dB$ (CGH@DeMUX) = 2.3 dB. The CGH is assumed to be realized as an 8-level phase-only diffractive element [9].

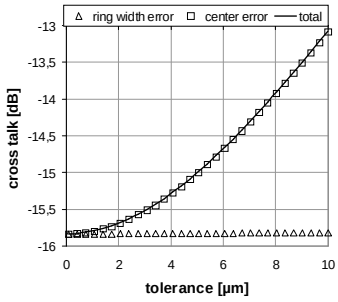

Fig. 4: Cross talk caused by the DeMUX (see text)

From the derived design data the volume consumption is $V_{MUX} \approx \pi 5^2 \cdot 8\ mm^3 \approx 0.6\ cm^3$ and $V_{DeMUX} \approx \pi 3^2 \cdot 8\ mm^3 \approx 0.25\ cm^3$ for the MUX and DeMUX modules, respectively.

References

[3] U. W. Krackhardt, R. Klug, K.-H. Brenner, Broadband parallel fiber optical link for short distance interconnection with multi-mode fibers, Appl. Opt. 39, No. 5, 690 - 697, (2000)

[8] R. Klug, U.W. Krackhardt, Influence of a Gaussian wave front on the angular spread through multimode step-index fibers , this report

[9] U. Krackhardt, N. Streibl, J. Schwider, Fabrication errors of computer generated multilevel phase-holograms, Optik 95, No. 4, 137 - 146, (1994)

7 Design and investigation of a refractive Gaussian to flat-top converter

Peter Kümmel, Karl-Heinz Brenner

For the next generation of DVD we have designed an Gaussian to flat-top converter that increases the light efficiency in the optical pick-up from about 25 % up to 100 % (fig. 1). This converter uses two refractive optical elements (fig. 2).

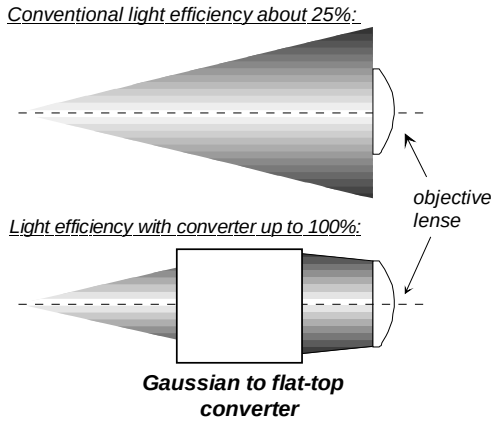

Fig. 1 Improved light efficieny by beam shaping

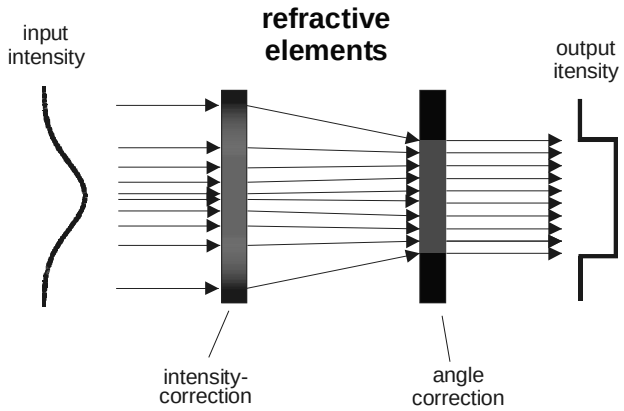

Fig. 2 Geometric model of the Gaussian to flat-top converter

The design method is based on conservation of energy of geometrical rays and the thin-element approximation (TAE). This approach leads to an analytically solvable equation for the optical phase of the first element which was solved numerically by integration. For an experimental verification of the design procedure, we chose the situation of a Gaussian beam width of 1.5 *mm*, position of the second element in a distance of 60 *mm* and a top-hat radius of 2.2 *mm* with a theoretical power efficiency of 99 %. Fig. 4 shows the radial phase distribution of the element resulting from these parameters, it also shows the measured phase of the realized element. The element was fabricated by direct write in photo resist (IOF Jena). The properties of the designed element were analyzed by numerical nonparaxial wave-propagation as well as by experimental characterization. Fig. 5 shows the calculated output intensity as a gray-level image. Fig. 6 shows the measured output intensity.

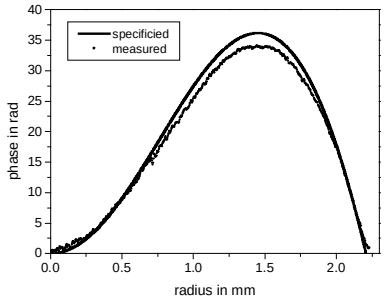

Fig. 3 Phase of the beam shaping element as a function of radius

Fig. 4 Gray-level image of calculated output intensity

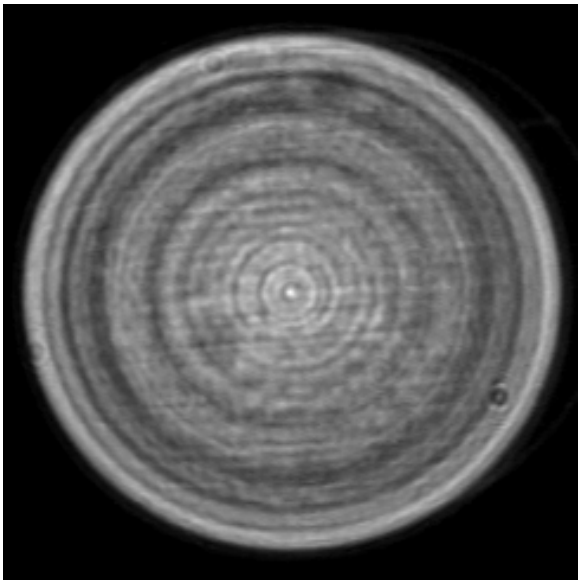

Fig. 5 Gray-level image of measured output intensity

References

[10] P. Kümmel, U. Krackhardt, K.H. Brenner. Berechnung und Herstellung mikrooptischer Elemente für den blauen DVD-Standard. Optik in der Rechentechnik, Hagen (2000)

8 Diffractive element for focus & position tracking in DVD-pickups by a Foucault knife-edge technique

S. Dambach [1], *U. W. Krackhardt*

In the scope of an European research project (BLUE-SPOT) our group is working on the optical pickup system of the next-generation DVD storage. By reducing the wavelength to 405 *nm* (blue), using fast front lenses and decreasing the pit size on the medium the capacity will be increased by a factor of more than 4 as compared to todays DVD $(4.7\ GB)$ systems.

One of our research goals is to provide a means for generating optical signals for track and focus error which can be subsequently evaluated in an electronic control circuit. Together with our industrial partner we realized a diffractive structure which in essence acts as aperture splitter and space variant deflector. The structure is partitioned into 4 quadrants each having a linear binary phase-only diffraction grating with individual size and orientation of the grating vectors (fig. 1). The grating is located in the converging backward beam of the pickup such that all quadrants are equally illuminated if the system is on track. The diffractive structure is designed such that the diffraction orders impinge on a structured detector.

In the case of perfect focus the, say, -1^{st} diffraction orders lie just between two adjacent detector areas (fig 2b). If the system is out of focus the image no longer coincides with the detector plane. The quadrant boarders of the diffractive element act as knife-edges. Thus, the direction of the rays constituting the focus are not symmetric with respect to the principal propagation direction. This leads to defocus patterns which show different orientations depending on the sign of the defocus (figs. 2 a, c). The control signal is obtained by electrically subtracting the voltages of adjacent detector areas. By the absolute value and the sign of the resulting voltage the amount and the direction of defocus can be monitored.

The track signal can be obtained in a similar manner: If the track is shifted out of focus, the quadrants of the diffractive structure are unequally illuminated. This changes the intensity distribution of the, say, $+1^{st}$ diffraction orders. Again, by electrically subtracting the voltages of corresponding detector areas, a monitoring signal for track control can be obtained.

For the fabrication of the diffractive structure we developed a polygon intersection algorithm to automatically generate structure data for our direct writing laser machine. The specifications were met with an absolute error of below 2 %. Technical assistance of the Fern-Universitt Hagen for etching the glass wafer is gratefully appreciated.

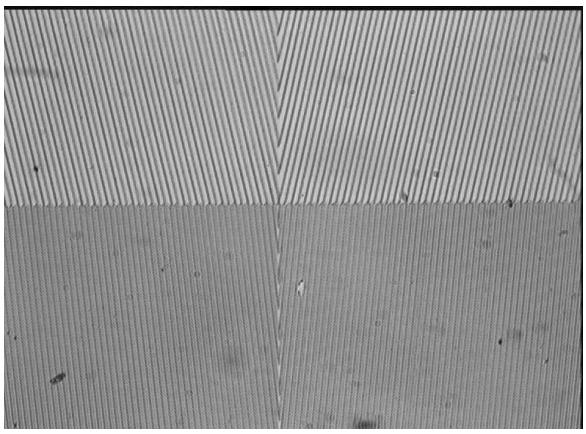

Fig. 1 Microscope image of the diffractive element

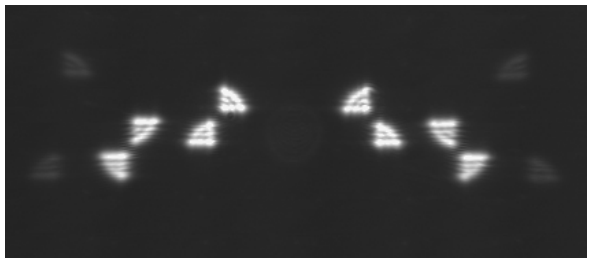

a) medium too near to front lens

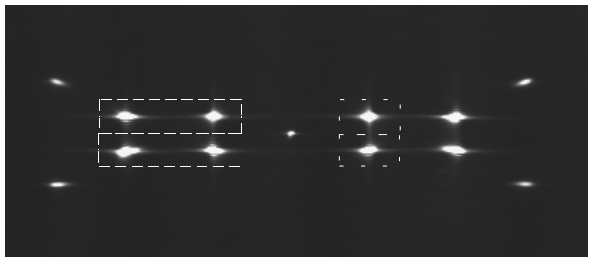

b) medium in focus (focus detector dashed, track detector dotted)

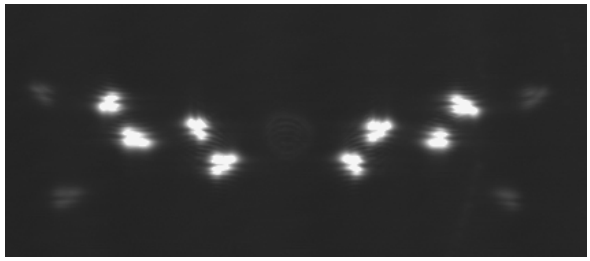

c) medium too far away from the front lens

Fig. 2 Diffraction pattern of diffractive element

[1] Thomson Multimedia GmbH, Hermann-Schwer-Str. 3, 78003 Villingen-Schwenningen

9 High NA - lens: Fresnel transmission and vector propagation

Peter Kümmel, Karl-Heinz Brenner

The next generation of DVD will have an objective lens / lens-system with about $NA = 0.85$. Figure 1 shows the corresponding angle aperture of $\arcsin(0.85) = 58^o$. Refraction at such large angles makes an investigation necessary considering the polarization of the incident ray. In a single lens-system there are two points of refraction: 1. air-lens and 2. lens-air, see Fig. 1. At these points are light losses described by Fresnels formulae. Because of different transmissions of the three electromagnetic components, the refraction will also change the direction of polarization. We have calculated the intensity losses and rotation of polarization for such a system. Using a lens diameter of 5 *mm* and $n = 1.5$ for the lens refractive index we assume a incident linear polarized plane wave with the only non vanishing x-component of the electromagnetic field. Figure 2 shows the intensity transmission of the two following refractions. The two maxima origins in the Brewster angles.

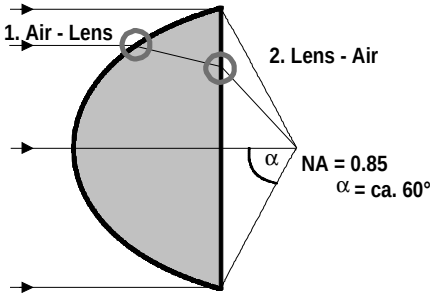

Fig. 1: High NA lens.

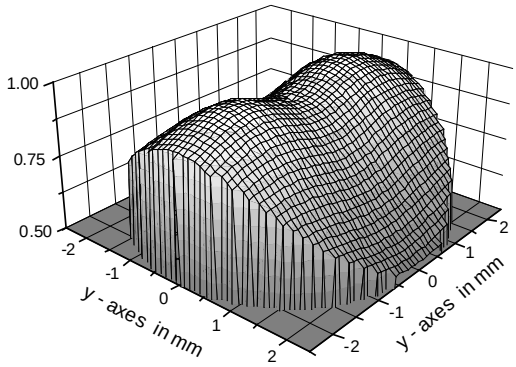

Fig.2: Intensity transmission of the lens.

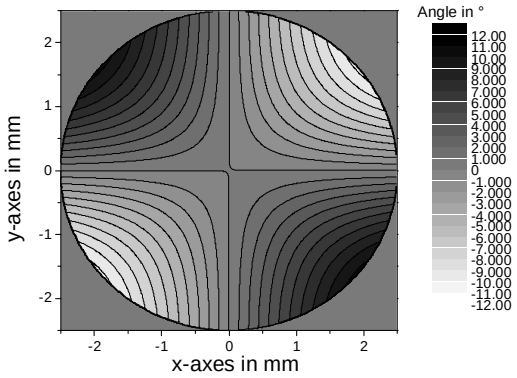

Fig.3:Rotation of polarization. (Angle: -12^o to 12^o)

Of high interest is the intensity distribution in the focal plane. Therefore we have calculated this distribution under considering the vector character of light. The validity of ray-tracing breaking down at such high NA we use a wave optical description. The downward propagation was calculated for the three component separate by the Kirchhoff diffraction integral. Summation of the three individual intensity distributions gives the overall intensity. Figure 4 shows the calculated intensity distributions of the three components (aplanatic lens, $NA = 0.85$, $\lambda = 405\ nm$).The no more longer rotational symmetric overall amplitude distribution of the electric field shows Fig. 5. The added circle indicates the first minimum of the scalar diffraction theory (Airy).

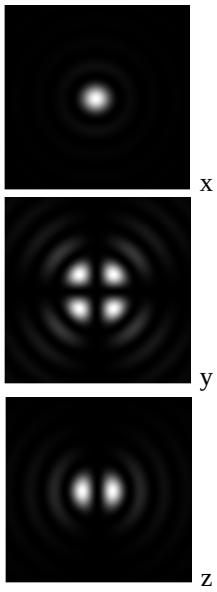

Fig. 4: Intensity of the three components

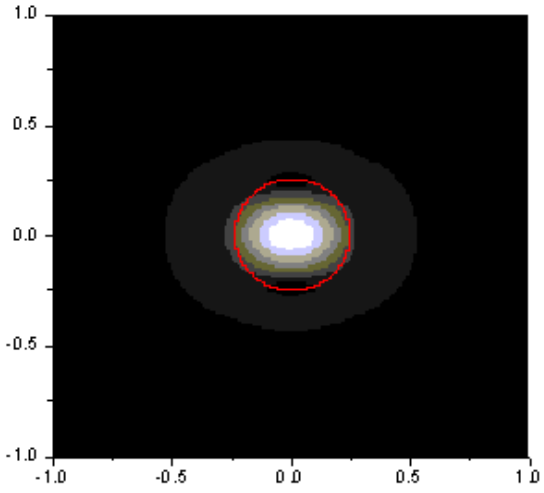

Fig. 5: Overall intensity in focal plane of a NA=0.85 system. Units in μm.

10 Equivalence of paraxial optical systems

K.-H. Brenner, W.T. Rhodes[1]

On the occation of a visit to Mannheim last year, Bill Rhodes, the director of research at Georgia Tech Lorrain in Metz, France posed an interesting problem, for which he provided a closed solution. The problem can be stated like this: Is it possible to realize diffraction in free space over a distance of z with an optical system that is much shorter than z ? In a mathematical formulation, the goal is to find an equivalent, but shorter optical system which realizes a Fresnel transformation. The solution Bill came up with [11] consisted of two lenses, a scaling unit, and free space propagation over a distance

$$z_s = \frac{zf}{z+f},$$

which is obviously shorter by a factor

$$\frac{z_s}{z} = \frac{f}{z+f}.$$

By employing diffraction integrals he was able to prove that this system was mathematically equivalent to a Fresnel transformation.
Using the Wigner description of optical systems, the same proof can be performed by linear transformations in phase-space. In Wigner-space, the effect of propagation (P), a lens (L), and scaling (S) are described by the matrices

$$P(z) = \begin{pmatrix} 1 & z \\ 0 & 1 \end{pmatrix} \quad L(f) = \begin{pmatrix} 1 & 0 \\ -\frac{1}{f} & 1 \end{pmatrix} \quad S(m) = \begin{pmatrix} m & 0 \\ 0 & \frac{1}{m} \end{pmatrix}$$

with z as the propagation distance, f as the focal length and m as the scaling factor. These matrices act on phase space coordinates

$$\vec{r} = \begin{pmatrix} x \\ k_x \end{pmatrix}$$

and are readily identified as the ray-transfer matrices, known in paraxial optics. While rays are only applicable in the eikonal approximation, the identification of phase-space coordinates as generalized rays was shown to be mathematically equivalent to the integral treatment of quadratic optical systems [12] if a description in terms of the complex amplitude was replaced by a description in terms of the Wigner function.
The above solution can be expressed in terms of system matrices by the equality

$$L(-z-f)S\left(\frac{z+f}{f}\right)P\left(\frac{zf}{z+f}\right)L(f) = P(z),$$

which must be read from right to left. A lens with focal length f is placed behind the complex amplitude u_0. Then a propagation over a distance $zf/(z+f)$ follows. The result is scaled and a second lens with negative focal length is applied. This concept can be extended also to other problems. A problem of special interest was a focusing system. The equality

$$S\left(\frac{1}{\sqrt{m}}\right)P(mf)L(mf)S\left(\sqrt{m}\right) = P(f)L(f)$$

states that a focusing system consisting of a lens (f) and a propagation distance (f) can be replaced by a scaled system (factor m) if the input is scaled by $\sqrt{m}$ and the output is scaled by $\sqrt{1/m}$.

References

[11] W.T. Rhodes, Seminar Presentation “ Light tubes, Wigner diagrams, and numerical simulation of Fresnel propagation “ presented at University of Mannheim, 2000
[12] M.J. Bastiaans, Optica Acta 26 (1979) 1265, J. Opt. Soc. Am 69 (1979) 1710.

[1]Georgia Tech, Lorraine, Metz, France

11 Correct sampling of paraxial focusing systems

K.-H. Brenner

Since the class of analytically solvable problems is much smaller than the class of all problems, there is always a need for numerical methods in order to solve those problems, where an analytic solution cannot be derived. For a satisfactory numerical representation, the continuous distribution has to be sampled according to the Nyquist criterion, stating that the sampling distance

$$\delta x \leq \frac{1}{2\nu_{max}}$$

has to be smaller that a half of the period of the highest frequency. Optical systems consist of lenses and propagation distances. In the paraxial approximation, these modules can be approximated by quadratic systems. Thus a thin lens can be described by a quadratic phase factor. The real (or imaginary) part of the lens amplitude is a sinusoidal function with linearly increasing spatial frequency:

$$\nu(x) = \frac{x}{\lambda f}$$

Hence, correct sampling of a lens with diameter $D = 2R$ requires that

$$\delta x_{lens} \leq \frac{\lambda f}{2R}$$

Thus the sampling has to be better than the spot-size λ/NA for a numerical treatment of lenses. If we use N sampling points to represent the input diameter, the relation $2R = N\delta x$ indicates that

$$f \geq \frac{N\delta x^2}{\lambda}$$

is a necessary requirement for the focal length of the lens. The propagation in space in the Fresnel approximation can be solved most easily in the Fourier plane, where the spatial frequency spectrum is multiplied by the quadratic phase $\pi\lambda z\nu^2$. By similar steps we find that the sampling in the frequency domain according to Nyquist requires that

$$\delta\nu_{propagation} \leq \frac{1}{2\lambda z\nu_{max}}$$

Using a discrete Fourier transform, the spatial and the frequency sampling are related by $\delta\nu = 1/N\delta x$, thus $\nu_{max} = 1/2\delta x$ and we observe the condition

$$z \leq \frac{N\delta x^2}{\lambda}$$

for the propagation distance. Thus, if lens- and propagation modules are chained, the Nyquist criterion requires that

$$z \leq \frac{N\delta x^2}{\lambda} \leq f$$

leaving

$$z = \frac{N\delta x^2}{\lambda} = f$$

as the only option for a focusing system with a full lens diameter.

12 Off-axis operation of optical phase elements

K.-H. Brenner

A hologram is typically reconstructed by illuminating it with a plane wave from a collimated laser and observing the reconstruction at the focal plane of a lens. For a binary phase hologram, the zero diffraction order can be suppressed, if the phase difference between the two levels is π , or equivalently, if the difference between the two height levels is

$$\frac{\lambda}{2(n-1)}$$

.

If the hologram is placed in the collimated beam not perpendicular to the axis, but at an off-axis angle, the light path through the phase element will become longer by a factor $1/\cos\vartheta$. Therefore it is a widely held believe, that also the phase levels *h* will increase by this factor and the phase will be $\phi_{off-axis} = k(n-n_0)\frac{h}{\cos\vartheta}$. To make things short, this formula is wrong and Markus Testorf and Wolfgang Singer, two former PhD-students during my time in Erlangen were puzzled by this, comparing it with the Rayleigh-Sommerfeld propagation, described by

$$u(\vec{r_\perp},z) = \frac{1}{(2\pi)^2}\int\int \tilde{u}\left(\vec{k_\perp}\right) e^{i\vec{k_\perp}\vec{r_\perp}} e^{iz\sqrt{\left(\frac{n\omega}{c}\right)^2 - k_\perp^2}} d^2k_\perp$$

It indicates, that e.g. for the *x*-component, $k_x = nk_0\sin\vartheta$ and thus

$$z\sqrt{\left(\frac{n\omega}{c}\right)^2 - k_\perp^2} = k_0 z\sqrt{n^2 - n^2\sin^2\vartheta} = k_0 zn\cos\vartheta$$

is the appropriate phase factor, to be applied if a plane wave propagates in a medium with index *n* at an off-axis angle ϑ . Since there is a significant difference between a factor $1/\cos\vartheta$ and the factor $\cos\vartheta$, Markus Testorf has pursued this problem, pointing out in a recent publication [13], that the correct phase factor for off-axis operation of a phase element with height *h* is

$$\phi_{off-axis} = k_0(n\cos\vartheta - n_0\cos\vartheta_0)h \tag{1}$$

if n_0 is the index of the outside medium, ϑ_0 is the angle of the illuminating plane wave outside and $\sin\vartheta = \frac{n_0}{n}\sin\vartheta$ is the angle of the plane wave inside the medium with index *n* . It is easy to show that eq. 1 can equivalently be written as

$$\phi_{off-axis} = k_0 h\left(\sqrt{n^2 - n_0^2\sin^2\vartheta_0} - n_0\cos\vartheta_0\right)$$

illustrating, how the Rayleigh-Sommerfeld description can be applied for propagation in an inhomogeneous medium.

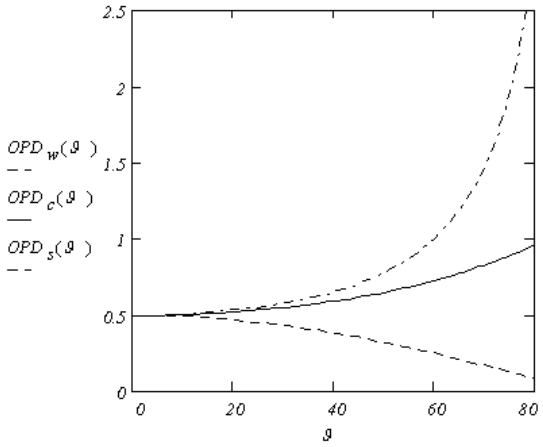

By using only ϑ_0 in the description, the initial spatial frequency spectrum can be used throughout the propagation in different media with different indices of refraction. The graph above shows the optical path length for $1/\cos\vartheta$ (top curve), $\cos\vartheta$ (bottom curve) and the correct formula (solid line) for an index difference of 0.5. It indicates that the phase indeed grows for off-axis angles and that the wrong formula (top) is an unexpectedly good approximation for the correct formula.

References

[13] M. Testorf, "On the zero-thickness model of diffractive optical elements", JOSA A 17, pp 1132-1133, 2000

13 Realisation of vertical coupling devices with SU-8 resist

J. Bähr, T. Schmelcher, K.-H. Brenner

We report the realization of multimode wave guide substrates for vertical coupling [14][15] with a very cost efficient UV-structuring technique in thick photoresist.
For realization of D-WG structures we suggest 3 different approaches. The first is to emboss a semi cylindrical structure into a blank of PMMA (fig. 1). After that the structure is filled with a high index material, for example Polycarbonate. The second approach is the field assisted silver-sodium ion exchange process in planar glass substrates [16]. Here we use soda-lime glasses coated with a thin layer of Titanium which is structured on one side by a photolithographic process. This glass is put into a silver salt melt at a temperature of about 250 to 400 degrees. Between the melt and the bottom of the glass an electrical field is applied, which forces the silver ions from the melt into the glass. In case of a line shaped mask with a very narrow aperture, next to the mask aperture the electrical drift field shows semi cylindrical geometry in good approximation [3]. According to the ion migration alongside the drift lines the index distribution is semi cylindrical, too. This approach is certainly the most expensive one. But the main advantage is that by applying a post heating process, the step like index distribution can be smoothened, and even parabolic distributions can be attained with high precision [16]. With this technique we can get step-index and also graded-index profiles to reduce modal dispersion.
The third approach is the most cost efficient. We realized strip-wave-guides by UV-structuring of thick photo resist (SU-8 by MicroresistTM). By varying the rotation speed of the spinning machine we can adjust the thickness between 10 to approximately 1000 microns with good repeatability. With $2000 U/min$ thickness of 50 ± 5 micron could be obtained. The index of the resist is 1.61 . After UV-exposure the non exposed areas can be unhinged so we can attain rectangular shaped strip waveguides.

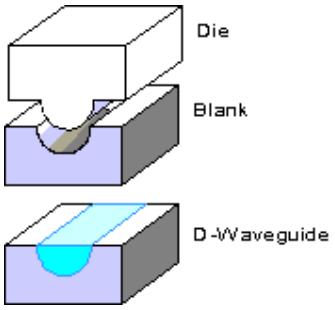

fig. 1 emboss and fill: step-index profiles

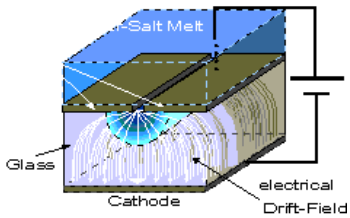

fig. 2 field assisted ion exchange process: step index and also graded profiles

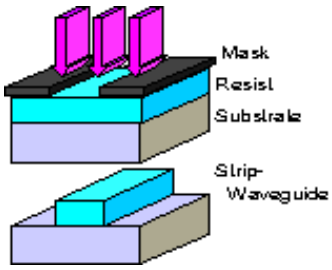

fig. 3 UV-structuring of thick resist: strip waveguides with step index profile

We realized plug on top coupling with these strip wave-guides. According to figure 4 we put two identical substrates on top of each other. Light was coupled into the bottom wave-guide. The microscope image of the back surface demonstrates the energy transition into the upper substrate. For better visualization of the two strip-wave-guide substrates a slight shear between the substrates was introduced. The height of the strip-wave-guide was 40 μm, his width was 100 μm. The substrates were pressed together with a force of approximately 1 N/cm^2. We did not use any index matching for this experiments. Since the modes are distributed statistically in multi mode wave guides, the maximum amount of energy transition is limited to 50%. In our first experiments we obtained an transition of $44 \pm 5\%$ of the inserted energy. By comparing the power in both wave-guides in the plugged situation with the power in the bottom wave-guide without connection we obtained a coupling loss of about 0.05 dB.

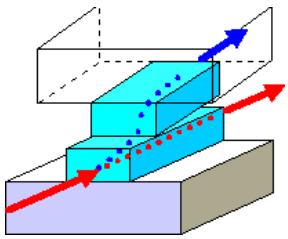

fig. 4 scheme of the vertical coupling of two strip waveguide substrates

fig. 5 microscope image of the output planes of the strip waveguides

Refereces

[14] T.Schmelcher, Jochen Bähr, K.-H. Brenner. Fabrication of integrated D-Waveguide Y-Branches by field assisted ion-exchange. Annual Report 1999, page 4
[15]
[16] J. Bähr, K.-H. Brenner. H-ROD a new and versatile microoptical component Optik 2000, accepted

14 Experiment for measuring wavelength and angle tolerance of two dimensional continuous phase elements

G. Walze

Diffractive elements can be used for many of today's applications. One goal in designing diffractive elements is to obtain a high diffraction efficiency. Therefore phase-only elements are preferred to amplitude elements. The diffraction efficiency increases with the number of phase quantization levels. Therefore continuous phase elements (CPEs) are expected to show the highest diffraction efficiency. With a new design method [17] we are now able to design arbitrary two-dimensional continuous phase elements. Our goal is to investigate the tolerance of elements designed with this method against changes in wavelength and incident angle. In order to measure this tolerance, we build a test arrangement in which wavelength and angle can be varied.

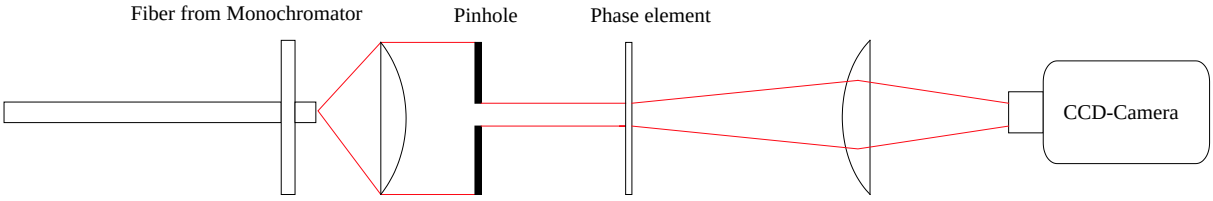

The wavelength can be varied from 480 $nm - 840\ nm$ and the angle from $-60^o to + 60^o$. The first test object reconstructs an arrangement of 24 spots representing the letters UM for University of Mannheim.

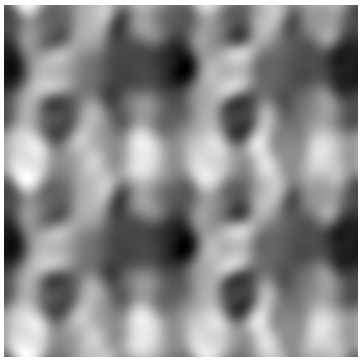

Fig. 1 Continuous Pahse Distribution

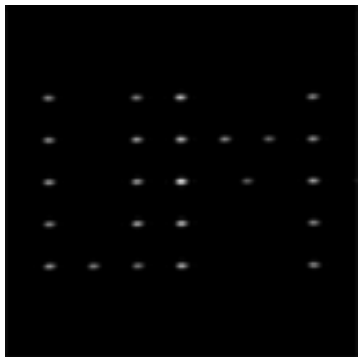

Fig. 2 Reconstructed Intensity

Figure 1 shows the continuous phase element, where different greyscales are representing different phase values. The phase change of this element covers a range of $2,51 \cdot \pi$. The whole element had all together 5*5 of these patterns tiled in a $2\ mm * 2mm$ square. Figure 2 shows the reconstructed image on a CCD-Camera. The centrer spot corresponds to the zero diffraction order.

The diagrams below show the first results of the experiment. The diagrams are showing the standard deviation of the spots relative to their middle value for wavelength (Fig. 3) and angle (Fig. 4). Because the element is designed to be homogeneous at the design wavelength, a minimum is expected for this wavelength. In our experiments we found that this deviation is a reliable measure of wavelength- and angle tolerance.

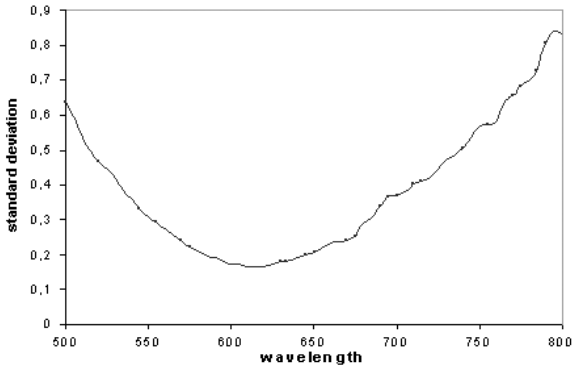

Wavelength dependence of standard deviation

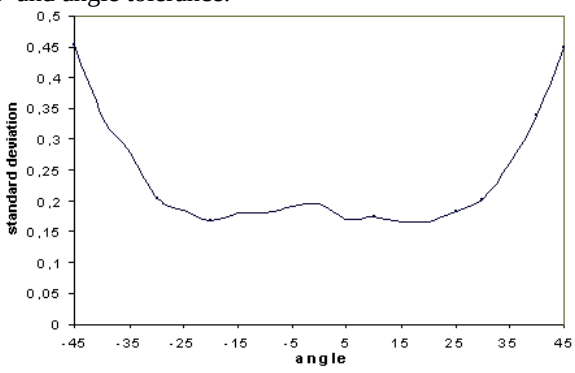

Angle tolerance of the standard deviation

References

[17] K.-H. Brenner. Method for designing arbitrary two-dimensional continuous phase elements *Opt. Lett.* 25, 31-33 (2000)

15 Measurement of the attenuation of D- Waveguides by cut-back method

T. Schmelcher, J. Bähr, S. Serov

For optical interconnects at the board-board and chip-chip level, there is an increasing interest in solutions, which are tolerant with respect to fabrication, positioning and operation conditions. Consequently multimode interconnects are favored over single-mode approaches in the short distance regime. The interconnection system we proposed earlier [18], utilizes D-shaped multimode waveguide structures, which are embedded in a planar substrate. The flat side of the D-structure is realized as the substrate surface and completes virtually the structure to a full cylindrical by total internal reflection (Fig. 1a). In analogy to D-fibers [19] we use the expression D-waveguides (D-WG).

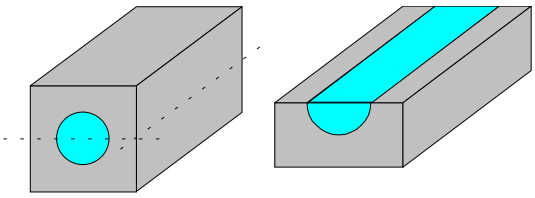

Fig. 1a An integrated Rod is structurally equivalent to a semi-cylinder due to total internal reflection at the surface

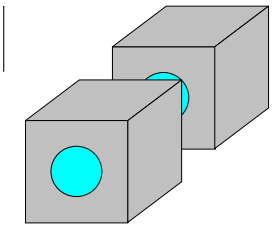

Fig. 1b Front-end coupling

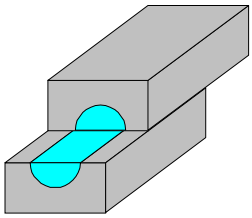

Fig. 1c Plug-on-top coupling

Due to this D-WG structure all the operations of guiding and beam splitting can be realized. In addition to front-end coupling one can easily realize a plug-on-top coupling by simply placing a second D-WG on top. For the realization of D-WG structures, different techniques can be applied. One possibility would be to emboss a structure into a polymer and to fill the resulting channel with a higher index polymer. In the present stage we use the field assisted silver-sodium ion exchange process in planar glass substrates and direct write techniques [20]. These processes provide step or graded index variations [21] [22]. Coupling into the D-waveguide was realized by focusing a laser at the front surface. The back surface was monitored by a microscope setup with a CCD camera and a power meter.

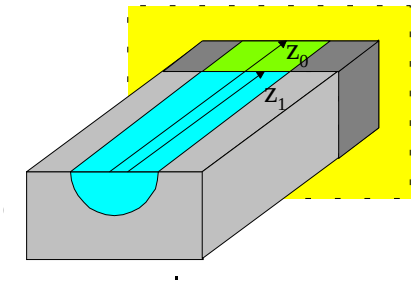

Fig. 2 Measurement–principe

D-Waveguide	1	2	3	4	5	6	Average
Power / mW @ $z_0 = 26.65\ mm$	35.6	39.2	38.0	37.5	35.0	36.0	36.9
Power / mW @ $z_1 = 15.93\ mm$	50.0	53.8	52.8	50.3	48.6	48.8	50.7
a dB/cm	1.38	1.28	1.33	1.19	1.33	1.23	1.29

A large part of this attenuation is due to normal glass-attenuation, which contributes at the measurement wavelength to . By choosing a different wavelength and / or a different glass type the attenuation can be reduced . The remaining attenuation can be explained by micro cracks and non- uniform exchange regions.

References

[18] T. Schmelcher, J. Bähr, K.-H. Brenner. Tolerant coupling of integrated Multimode Waveguides *LEOS*, Vol.2 , 571–572 (2000), San Juan.

[19] F. Mackenzie, R. Payne. D-fibre optical backplane interconnect. In *Proc. of SPIE*, **2153**, 218–226 (1994).

[20] J. Bähr, T. Schmelcher, K.-H. Brenner. D-WG-SU8 page 7 Annual Report 2000.

[21] H.-J. Lilienhof, E. Voges, D. Ritter, B. Pantschew. Field-induced index profiles of multimode ion-exchanged strip waveguides. *IEEE Jour. of Quantum Electronics*, **18**, 1877–1883 (1982)

[22] J. Bähr, K.-H. Brenner.Realization and optimization of planar refracting microlenses by Ag–Na ion–exchange techniques. *Appl. Opt.*, **35**, 5102–5107 (1996)

A List of recent publications

68. K. - H. Brenner, U. Krackhardt. Komponenten und Aufbautechniken für mikro-optische Systeme zur Informationsübertragung und -verabeitung. *it+ti*, **41**, 39–48 (1999)

69. R. Klug, U. Krackhardt, K.-H. Brenner. Richtungsmultiplex für optische Verbindungen zwischen Platinen. Tagungsbeitrag ORT 98 Paderborn.

70. D. Dragoman, M. Dragoman, J. Bähr, and K.-H. Brenner. Phase space measurements of micro-optical objects. *Applied Optics*, **38**, 5019–5023 (1999)

71. R. Klug, U. W. Krackhardt, K.-H. Brenner. Angular Multiplexing for optical Board to Board Interconnections. In Optics in Computing, OSA Technical Digest, 11, page 8 - 120, Snowmass 1999.

72. U. Krackhardt and K.-H. Brenner. The berry-phase applied to optical metrology. In *Verh. der DPG*, page KY 5.3 (1999) ISSN 0420-0195.

73. D. Dragoman, M. Dragoman and K.-H. Brenner. Experimental Demonstration of a continuously variant fractional Fourier Transformer. *Applied Optics*, **38**, 4985–4989 (1999)

74. R. Klug and K.-H. Brenner. Implementation of multilens micro–optical systems with large numerical aperture by stacking of microlenses. *Appl. Opt.*, **38** 7002–7008 (1999)

75. D. Dragoman, M. Dragoman and K.-H. Brenner. Variant fractional fourier transformer for optical pulses. *Opt.Lett.*, **24**, 933–935 (1999)

76. K.-H. Brenner, R. Klug and U.W. Krackhardt. Angle division multiplexing in multi-mode fibers for optical board-to-board interconnection. *SPIE*, eds P.Réfreègier, B. Javidi, Euro-American Workshop on Optoelectronic Information Processing, Critical Review, **CR74**, 61–69 (1999)

77. U.W. Krackhardt, R. Klug and K.-H. Brenner. Broadband parallel-fiber optical link for short-distance interconnection with multimode fibers. *Appl. Opt.*, **39**, 690–697 (1999)

78. K.-H. Brenner, R. Klug and A. Knüttel. Microoptic Implementation of an Array of 1024 Confocal Sensors. In *OPTO '98 Proceedings*, AMA Fachverband für Sensorik, 155–160, Erfurt 1998.

79. K.-H. Brenner, U.W. Krackhardt and R. Klug. Directional Multiplexing for optical Board to Board Interconnections. In *Proc. of SPIE*, Optics in Computing '98, **3490**, 416–418, Bruegge 1998.

80. J. Bähr and K.-H. Brenner. Optical motherboard: a planar chip to chip interconnection scheme for dense optical wiring. In *Proceedings of SPIE*, Optics in Computing '98, **3490**,419–422, Bruegge 1998.

81. K.-H. Brenner. Analysis of phase anomalies and design of continuous phase elements. *Diffractive Optics '99*, EOS Topical Meeting Digest Series, 22:163–164 ISSN 0420-0195, Jena 1999

82. U. Krackhardt and K.-H. Brenner. Forward construction of hoes by continuous aperture division. In *Proc. Diffractive Optics*, pages 163–164, 1999. ISSN 1167-5357.

83. K.-H. Brenner. Method for designing arbitrary two–dimensional continuous phase elemnts. *Opt. Letters* **25**, 31–33 (2000)

84. U. W. Krackhardt, R. Klug and K.-H. Brenner. Faser–optische Kurzstreckenverbindungen zur breitbandigen und parallelen Signalübertragung Tagungsbeitrag ORT 99 Jena, Band 4, 1999.

85. J. Bähr, K.-H. Brenner, J. Moisel, W. Singer, S. Sinzinger, T. Spick and M. Testorf. Modification of the imaging properties of ion-exchange microlenses by mask shaping In *Technical Digest of the Tenth Topical Meeting on Gradient-Index Optical Systems*, EOS 1992, p. 187, Santiago de Compostela, Spain, 4.-6. Oct. 1992

86. K.-H. Brenner U. Krackhardt. Flächenhaftes Interferometer. patent pending, DE 198 33 291 A1,IPC G01B 9/02, 1998.

87. U. W. Krackhardt, R. Klug, K.-H. Brenner Demonstration of a parallel optical transmission using angle multiplexing in optical fibres *Optics in Computing 2000* Roger A. Lessard, Tigran Galstian, Editors, Proceedings of SPIE, Vol. 4089, 86 - 92, ISBN 0-8194-3732-8, ISSN 0277-786X, Quebec City, Canada (2000)

88. K.-H. Brenner, J. Bhr, T. Schmelcher Design and Fabrication of arbitrary , non-separable continuous phase elements in *Diffractiv Optics and Micro-Optics*, OSA Technical Digest, 237 - 239, ISBN 1-55752-635-4, Quebec City, Canada (2000)

89. U. W. Krackhardt, R. Klug, and K.-H. Brenner Multimode Fiber Interconnect for Parallel, High Bandwidth - Short Distance Data Link in *Progress in Electromagnetics Research Symposium* (PIERS), The Electromagnetics Academy, PIERS 2000 Proceedings, 726, ISBN 0-9679674-0-6, Cambridge, Massachusetts, USA (2000)

90. Daniela Dragoman, Mircea Dragoman, and Karl-Heinz Brenner Optical realization of the ambiguity function of real two-dimensional light sources *Applied Optics* 39, No. 17, 2912 - 2917, (2000)

91. Karl-Heinz Brenner Development of modules for micro optical integration and MOEMS packaging in *MOEMS and Miniaturized Systems*, Eds: M. Edward Motamedi, Rolf Gring, Proceedings of SPIE, Vol. 4178, 138 - 140, ISSN 0277-786X, Santa Clara, USA (2000)

92. P. Kümmel, U. Krackhardt, K.-H. Brenner, S. Dambach Berechnung und Herstellung mikrooptischer Elemente für den blauen DVD-Standard 5. Workshop Optik in der Rechentechnik, Tagungsband, eds.: Stefan Sinzinger, Jrgen Jahns, 69 - 73, ISSN 1437-8507, Hagen (2000)

93. U. W. Krackhardt, R. Klug, K.-H. Brenner Realistion and Application of a parallel high-bandwidth Interconnect over a single multimode Fibre by Angle Division Multiplexing in 14th International Conference on Optical Fiber Sensors, A.G. Mignani, H.C. Lefvre, Editors, *Proceedings of SPIE*, Vol. 4185, 174 - 177, ISSN 0277-786X, Venedig (2000)

94. J. Bähr, T. Schmelcher, K.-H. Brenner Tolerant Coupling of integrated Multimode Waveguides in *LEOS 2000*, IEEE Annual Meeting Conference Proceedings, Vol. 2, 571 - 572, ISBN 0-7803-5947-X, Puerto Rico (2000)

95. J. Bähr, K.-H. Brenner H-ROD: A new and versatile microoptical component OPTIK (2000), accepted

96. Jochen Bähr, Thilo Schmelcher, Karl-Heinz Brenner Tolerant Coupling of integrated Multimode Waveguides in *Optics in Computing*, OSA Technical Digest, 116 - 118, ISBN 1-55752-656-7, Lake Tahoe/Nevada (2001)

97. U. Krackhardt, R. Klug, K.-H. Brenner Angle Division Multiplexing: Investigation of the multiplexing potential of real systems *ORT 2001*, Proceedings 6th Workshop Optics in Computing Technology, 101 - 108, ISSN 1437-8507, Paderborn (2001)

98. T. Schmelcher, J. Bähr, K.-H. Brenner Tolerant Coupling of integrated Multimode Waveguides *ORT 2001*, Proceedings 6th Workshop Optics in Computing Technology, ISSN 1437-8507, 87 - 91, Paderborn (2001)

99. Karl-Heinz Brenner, Ulrich Krackhardt and Michael Kraft Integrated guiding structures for passive alignement of micro optical components *SPIE* 46. Annual Meeting, accepted

100. Jochen Bähr, Karl-Heinz Brenner Realization of refractive continuous phase elements with high design freedom by mask structured ion ex-change *SPIE* 46. Annual Meeting, accepted

101. Karl-Heinz Brenner, Peter Kümmel Design and Investigation of a Gaussian to flat-top converter for optical storage applications *SPIE* 46. Annual Meeting, accepted

Publisher: Lehrstuhl für Optoelektronik
Fakultät für Mathematik und Informatik
Universität Mannheim
B6, 23-29
D–68131 Mannheim
Germany

Tel: +49 (0)621 181–2700
Fax: +49 (0)621 181–2695
Mail: info@oe.ti.uni-mannheim.de
WWW: http://www.ti.uni-mannheim.de/~oe

Editor: Dipl.–Ing. Thilo Schmelcher

Tel: +49 (0)621 181–2693
Mail: t.schmelcher@oe.ti.uni-mannheim.de

Print: Universitätsdruckerei Mannheim

Literatur

[1] J. Ghozeil. *Hartmann and other screen tests*. John Whiley, New York, 1992. ed. D. Malacara.

[2] J. Bähr and K.H. Brenner. High precision micro-lenses for hartmann-shack wave front sensoring for applications in ophthalmology, 2000. Annual Report.

[3] U.W. Krackhardt, R. Klug, and K.-H. Brenner. Broadband parallel-fiber optical link for short-distance interconnection with multimode fibers. *Appl. Opt.*, 39:690–697, 2000.

[4] U.W. Krackhardt and S.M. Flammuth. Automated measurement of fiber quality for angle division multiplexing applications, 2000. Annual Report.

[5] D. Gloge. Optical power flow in multimode fibers. *Bell Syst. Techn. J.*, 51:1767–1783, 1972.

[6] R.Klug, U.W. Krackhardt, and H. Froening. Design of the demux unit for adm–based interconnects, 1999. Annual Report.

[7] R.Klug, U.W. Krackhardt, and S. Flammuth. Characterization of fiber parameters for angle division multiplexing, 1999. Annual Report.

[8] R. Klug and U.W. Krackhardt. Influence of a gaussian wave front on the angular spread through multimode step-index fibers, 2000. Annual Report.

[9] U. Krackhardt, N. Streibl, and J. Schwider. Fabrication errors of computer generated multilevel phaseholograms. *Optik 95*, 4, 1994.

[10] P. Kümmel, U. Krackhardt, and K.-H. Brenner. Berechnung ung herstellung mikrooptischer elemente für den blauen dvd-standard, 2000. Optik in der Rechentechnik, Hagen.

[11] W.T. Rhodes. Light tubes, wigner diagrams, and numerical simulation of fresnel propagation, 2000. Seminar presentation presented at University of Mannheim.

[12] M. J. Bastiaans. Method for designing arbitrary two-dimensional continuous phase elements. *J. Opt. Soc. Am.*, 69:1710, 1979.

[13] Markus Testorf. Method for designing arbitrary two-dimensional continuous phase elements. *JOSA*, 25:31–33, 2000.

[14] T. Schmelcher, J. Bähr, and K.-H. Brenner. Fabrication of integrated d–waveguide y–branches by field assisted ion–exchange, 1999. Annual Report.

[15] J. Bähr T. Schmelcher and S. Serov. Measurment of the attenuation of d-waveguides by cut-back method, 1999. Annual Report.

[16] J. Bähr and K.-H. Brenner. H-rod: A new and versatile microoptical component, 2000. OPTIK.

[17] K.-H. Brenner. Method for designing arbitrary two-dimensional continuous phase elements. *Optics Letters*, 25:31–33, 2000.

[18] T. Schmelcher, J. Bähr, and K.-H. Brenner. Tolerant coupling of integrated multimode waveguides. In *Proc. of Leos*, volume 2, pages 571–572, 2000.

[19] F. Mackenzie and R. Payne. D-fibre optical backplane interconnect. In *Proc. of SPIE*, volume 2153, pages 218–226, 1994.

[20] J. Bähr, T. Schmelcher, and K.-H. Brenner. Realisation of vertical coupling devices with su-8 resist, 2000. Annual Report.

[21] H.-J. Lilienhof, E. Voges, D. Ritter, and B. Pantschew. Field-induced index profiles of multimode ion-exchanged strip waveguides. *IEEE Jour. of Quantum Electronics*, 18(11):1877–1883, 1982.

[22] K.-H. Brenner J. Bähr. Realization and optimization of planar refracting microlenses by ag–na ion–exchange techniques. *Appl. Opt.*, 35:5102–5107, 1996.